Oncogene (2004) 23, 8171–8183

www.nature.com/onc

Gene expression profiling of advanced ovarian cancer: characterization of a molecular signature involving fibroblast growth factor 2

Loris De Cecco[1,2,3,6], Luigi Marchionni[1,6], Manuela Gariboldi[2,3], James F Reid[1,7], M Stefania Lagonigro[2,3], Stefano Caramuta[2,3], Cristina Ferrario[2,3], Erica Bussani[2,3], Delia Mezzanzanica[2], Fabio Turatti[2], Domenico Delia[2], Maria G Daidone[2], Maria Oggionni[4], Norma Bertuletti[4], Antonino Ditto[5], Francesco Raspagliesi[5], Silvana Pilotti[4], Marco A Pierotti*[,2,3], Silvana Canevari[2,8] and Claudio Schneider*[,1,8]

[1]Laboratorio Nazionale CIB, Area Science Park, Padriciano 99, 34012 Trieste, Italy; [2]Department of Experimental Oncology, Istituto Nazionale Tumori, via G Venezian 1, 20133 Milan, Italy; [3]IFOM FIRC Institute for Molecular Oncology, via Adamello 16, 20139 Milan, Italy; [4]Department of Pathology, Istituto Nazionale Tumori, via G Venezian 1, 20133 Milan, Italy; [5]Department of Surgical Oncology, Istituto Nazionale Tumori, via G. Venezian 1, 20133 Milan, Italy

Epithelial ovarian cancer (EOC) is the gynecological disease with the highest death rate. We applied an automatic class discovery procedure based on gene expression profiling to stages III–IV tumors to search for molecular signatures associated with the biological properties and progression of EOC. Using a complementary DNA microarray containing 4451 cancer-related, sequence-verified features, we identified a subset of EOC characterized by the expression of numerous genes related to the extracellular matrix (ECM) and its remodeling, along with elements of the fibroblast growth factor 2 (FGF2) signaling pathway. A total of 10 genes were validated by quantitative real-time polymerase chain reaction, and coexpression of FGF2 and fibroblast growth factor receptor 4 in tumor cells was revealed by immunohistochemistry, confirming the reliability of gene expression by cDNA microarray. Since the functional relationships among these genes clearly suggested involvement of the identified molecular signature in processes related to epithelial–stromal interactions and/or epithelial–mesenchymal cellular plasticity, we applied supervised learning analysis on ovarian-derived cell lines showing distinct cellular phenotypes in culture. This procedure enabled construction of a gene classifier able to discriminate mesenchymal-like from epithelial-like cells. Genes overexpressed in mesenchymal-like cells proved to match the FGF2 signaling and ECM molecular signature, as identified by unsupervised class discovery on advanced tumor samples. *In vitro* functional analysis of the cell plasticity classifier was carried out using two isogenic and immortalized cell lines derived from ovarian surface epithelium and displaying mesenchymal and epithelial morphology, respectively. The results indicated the autocrine, but not intracrine stimulation of mesenchymal conversion and cohort/scatter migration of cells by FGF2, suggesting a central role for FGF2 signaling in the maintenance of cellular plasticity of ovary-derived cells throughout the carcinogenesis process. These findings raise mechanistic hypotheses on EOC pathogenesis and progression that might provide a rational underpinning for new therapeutic modalities.

Oncogene (2004) **23,** 8171–8183. doi:10.1038/sj.onc.1207979
Published online 20 September 2004

Keywords: ovarian cancer; gene expression profiling; automated class discovery; epithelial–mesenchymal transition; epithelial–stromal interaction

Introduction

More patients die of epithelial ovarian cancer (EOC) than of any other gynecological disease. Despite relatively low morbidity, EOC presents a high case-fatality ratio, with overall 5-year survival still less than 30% (Greenlee *et al*., 2001). Women with organ-confined tumors have an excellent prognosis, but the majority of early-stage cancers are asymptomatic and more than two-thirds of patients are diagnosed with advanced disease (International Federation of Gynaecology and Obstetrics, FIGO stages III and IV) (Balli *et al*., 2000; Holschneider and Berek 2000). Clinical factors such as stage are related to tumor burden, which is likely to be a prognostic parameter; however, few biological characteristics have a proven prognostic role and the mechanisms by which they contribute to survival are unclear.

EOC is a morphologically and biologically heterogeneous disease, which has likely contributed to difficulties in defining the molecular alterations

*Correspondence: MA Pierotti, Department of Experimental Oncology, Istituto Nazionale Tumori, via G Venezian 1, 20133 Milan, Italy; E-mail: marco.pierotti@istitutotumori.mi.it; or
C Schneider; E-mail: schneide@sci.area.trieste.it
[6]These junior authors contributed equally to this work.
[7]Current address: IFOM FIRC Institute for Molecular Oncology, 20139 Milan, Italy.
[8]These senior authors contributed equally to this work.
Received 5 March 2004; revised 4 June 2004; accepted 4 June 2004; published online 20 September 2004

associated with its development and progression. Despite heterogeneous morphologies, all EOC subtypes originate from the single layer of epithelial cells covering the surface of the ovaries (ovarian surface epithelium, OSE cells). These cells share a common embryonic origin with epithelia of Mullerian duct-derived tissues, but differ from the granulosa-thecal cells of the ovary. Histopathological examination of clinical lesions has provided the evidence that ovarian epithelial cancer arises in the OSE (Feeley and Wells, 2001). OSE cells undergo repeated cycles of proliferation with the growth and rupture of ovarian follicles, and a well-characterized interaction between mesenchyme and epithelium dictates cyclical ovulation (Murdoch *et al*., 1992). Persistence and/or derangement of such microenviromental regulatory interactions might represent the basis of ovarian cancer progression, wherein molecular pathways, involving growth factors and hormones, might be critical. This notion is consistent with the high degree of plasticity retained by normal OSE cells, which can develop mesenchymal or epithelial phenotypes (Auersperg *et al*., 2001). In this respect, cell lines derived from OSE have provided a useful model in gene expression analysis (Matei *et al*., 2002).

The specific molecular mechanisms involved in the development of this disease have remained elusive. Alterations and/or amplification of p53, K-*ras*, HER-2/neu, c-*myc*, and many other genes have been reported in EOC, but the prevalence of these alterations depends greatly on case selection and is not ovarian-specific (Matias-Guiu and Prat 1998). Gain and loss of various chromosomal regions are common in EOC, but the target genes remain unknown (Shridhar *et al*., 2001).

Recent studies have reported the characterization of gene expression profiles of EOC and derivative cell lines (Hough *et al*., 2000; Hough *et al*., 2001; Tonin *et al*., 2001; Welsh *et al*., 2001). Molecular profiling has supported the likelihood that different subtypes represent distinct disease entities (Aunoble *et al*., 2000; Feeley and Wells, 2001), as demonstrated for the clear cell subgroup of EOC (Schwartz *et al*., 2002), and has suggested the use of detailed molecular information from tumor samples to enable identification of key downstream targets of signaling pathways (Schwartz *et al*., 2003). With respect to the identification of gene expression profiles associated with EOC carcinogenesis, sporadic EOC has recently been linked to the BRCA1 and BRCA2 pathways as possibly deregulated by epigenetic aberrations (Jazaeri *et al*., 2002).

In the present study, we focused on stages III–IV tumors with the aim of identifying molecular processes associated with this subset of EOC, which represents the most common clinical manifestation of the disease.

Results

Unsupervised class discovery and associated gene lists analysis

At initial diagnosis, tumors used in this study were predominantly characterized by advanced stage with a high-grade serous histology; 62% of the tumors exhibited p53 alterations (Table 1). These parameters were well in agreement with the more common clinical manifestation of this pathology. Hierarchical clustering analysis was used to explore data obtained by gene expression profiling of all 81 samples of the study, using a cDNA microarray containing 4451 cancer-related genes. This analysis revealed the aggregation of cancer specimens from the same patient, irrespective of the sampling site and consistent with the monoclonal origin of advanced disease (Tsao *et al*., 1993), supporting the high reproducibility of our data (see Supplementary section a). This approach also served to delineate several gene clusters characterizing distinct groups of samples, which were intermingled in the hierarchical tree, similar to recent observation by others (Schaner *et al*., 2003). Owing to the inherent deterministic limitations of hierarchical clustering, we used an automated class discovery approach, ISIS, to identify statistically

Table 1 Features of samples considered in the study

	No.
Samples	
Clinical specimens	
Ovarian tumors	
Tissue samples[a]	59
Cells from ascitic fluid[b]	6
Metastasis to ovary	5
In vitro cultures	
Normal/immortalized OSE	8
Ovarian carcinoma lines	3
Ovarian tumor patients[c]	
Stage	
Benign	1
Borderline	2
Early (I and II)	4
Advanced (III and IV)	43
Grade[d]	
1	4
2	5
3	36
NV	2
Histology[d]	
Serous	25
Endometrioid	12
Clear cell	2
Undifferentiated	8
P53 status[e]	
Wild type	16
Mutated	26

[a]In seven cases, multiple sampling was performed from different areas of the same primary tumor: OC5/OC20, OC13/OC42, OC15/OC81, OC40/OC80, OC46/OC77, OC48/OC60, OC62/OC85. In two cases, multiple sampling was performed from synchronous localizations: OC10/OC18 salpinx/ovarian, OC12/OC37/OC38 left ovarian/right ovarian/omental metastasis [b]Cells from six ascitic fluids were derived from five patients. In three cases a simultaneous sampling of the primary tumor was performed (tumor/ascites: OC26/OC71, OC28/OC72/OC73, OC29/OC69) [c]Total of 50 patients; median $\pm$ s.d. age in years, 53 ± 13 (range 20–76) [d]All 47 cases with malignant tumors [e]Cases (42) for which p53 status was determined

significant bipartitions of the samples based on their molecular signatures (von Heydebreck *et al*., 2001). This approach enables the generation of average gene expression profile sets by standard hierarchical clustering and determination of whether these profiles suggest one or more binary class distinctions of the samples. For each candidate bipartition obtained, the software then calculates a statistical score (diagonal linear discriminant, DLD) that quantifies the extent to which the two classes are separated by the expression levels of a suitable number of genes. We first applied ISIS on the whole matrix, identifying major splits corresponding to the different types of samples in this study (cells lines, ascites, and solid tumor samples) (data not shown). The 39 specimens of primary tumor from advanced disease, with the exclusion of the two clear cell cases, were used for the class discovery procedure (for class description, see Supplementary section b).

Gene list associated with ISIS binary partitions

To generate the list of genes responsible for sample partitioning, which is not produced as an output by ISIS, we applied a univariate *F*-test with a randomized variance model and FDR correction using BRB Array Tools (McShane *et al*., 2002; Radmacher *et al*., 2002). Among the gene lists generated by this approach, one was significantly enriched in genes related to the extracellular matrix (ECM), as assessed by the gene ontology (GO) terms distribution comparison made with the EASE software v.2.0 (Bonferroni corrected *P*-value <0.00059) (Hosack *et al*., 2003). The corresponding partition divided the samples in two groups of 21 and 18 tumors, respectively. The associated gene list consisted of 75 differentially expressed clones, corresponding to 74 different genes (Figure 1), which could be grouped into several functional categories. The largest functional category clearly contained numerous genes encoding structural proteins of the ECM (such as collagens and proteoglycans) and genes involved in cell adhesion and signaling. Notably, this list of genes also contained fibroblast growth factor 2 (FGF2), fibroblast growth factor receptor 4 (FGFR4), as well as other ECM-related genes reported to be regulated by FGF2 in various cellular contexts: OB cadherin (CDH11) (Strutz *et al*., 2002), lumican (LUM) (Long *et al*., 2000), biglycan (BGN) (Kinsella *et al*., 1997). At least two other functional categories were identified within the retrieved gene list, that is, several genes associated with the immune/inflammatory response of the host and various genes involved in transcription regulation (Supplementary section c), although they were not significant in terms of GO-terms distribution.

Real-time quantitative polymerase chain reaction (PCR) and immunohistochemistry validation

In total, 10 genes associated with the above-described partition were selected to validate gene expression levels measured by microarray analysis and analysed by quantitative real-time PCR (TaqMan), along with the reference RNA, in a representative subset of 18 EOC samples (nine displaying upregulation and nine exhibiting downregulation of the selected genes). The results were consistent with the relative expression data obtained by cDNA microarray for all 10 genes examined (Figure 2a).

To determine whether the observed gene expression pattern was reflected at the protein level, 22 tumors (12 displaying upregulation and 10 exhibiting downregulation of the chosen genes) were analysed immunohistochemically on multiple histologic sections with specific antibodies. Immunohistochemical analysis of FGFR4 is in keeping with published data (Valve *et al*., 2000); however, the intensity of labeling did not allow a clear partitioning of the samples. FGFR4 and FGF2 were both expressed at high intensity and restricted to tumor cells in all analysed samples, consistent with coexpression of the receptor and the growth factor. By contrast, fibronectin (FN1) immunoreactivity was present throughout the tumor samples, although restricted to the stroma and sparing epithelial components (Figure 2b).

Clinical associations

The ISIS partition discovered within tumor samples failed to associate with histotype, resistance to front-line chemotherapy, or TP53 status, and had no impact on patient survival (data not shown). By contrast, the gene composition of the classifier suggested the existence of an 'epithelial–mesenchymal plasticity' signature associated with this partition. Such an expression program might be related to the tissue of origin of EOC; in fact, normal OSE cells can actively differentiate along the mesenchymal or epithelial pathway (Auersperg *et al*., 2001). The following analyses were carried out to determine whether signature has biological significance.

Supervised learning of cultured ovarian cells

The cell lines profiled in our study displayed different cellular phenotypes in culture: cancer cell lines (IGROV1/OC52, platinum-resistant IGROV1 subline/OC54, OAW42/OC87) and the h-TERT cell line (OC104) evidenced epithelial and epithelial-like phenotypes, respectively, while OSE cells at the first *in vitro* passage (OC65, OC66) exhibited an intermediate phenotype, and OSE cells at the third *in vitro* passage (OC102, OC103, OC113) and the immortalized IOSE (OC67, OC112) displayed a more mesenchymal-like phenotype (Figure 3). It is well documented that OSE cells in culture can undergo epithelial–mesenchymal conversion, although with variable frequency and by still undefined mechanisms. Moreover, cultured OSE cells are highly responsive to environmental influences and may respond to the culture environment by modulating their state of differentiation. With passage in culture, the cells generally assume an increasingly definitive fibroblast-like phenotype as indicated by a change in polarity, reduced cell–cell adhesion, secretion of collagen, and loss of keratin expression (Auersperg

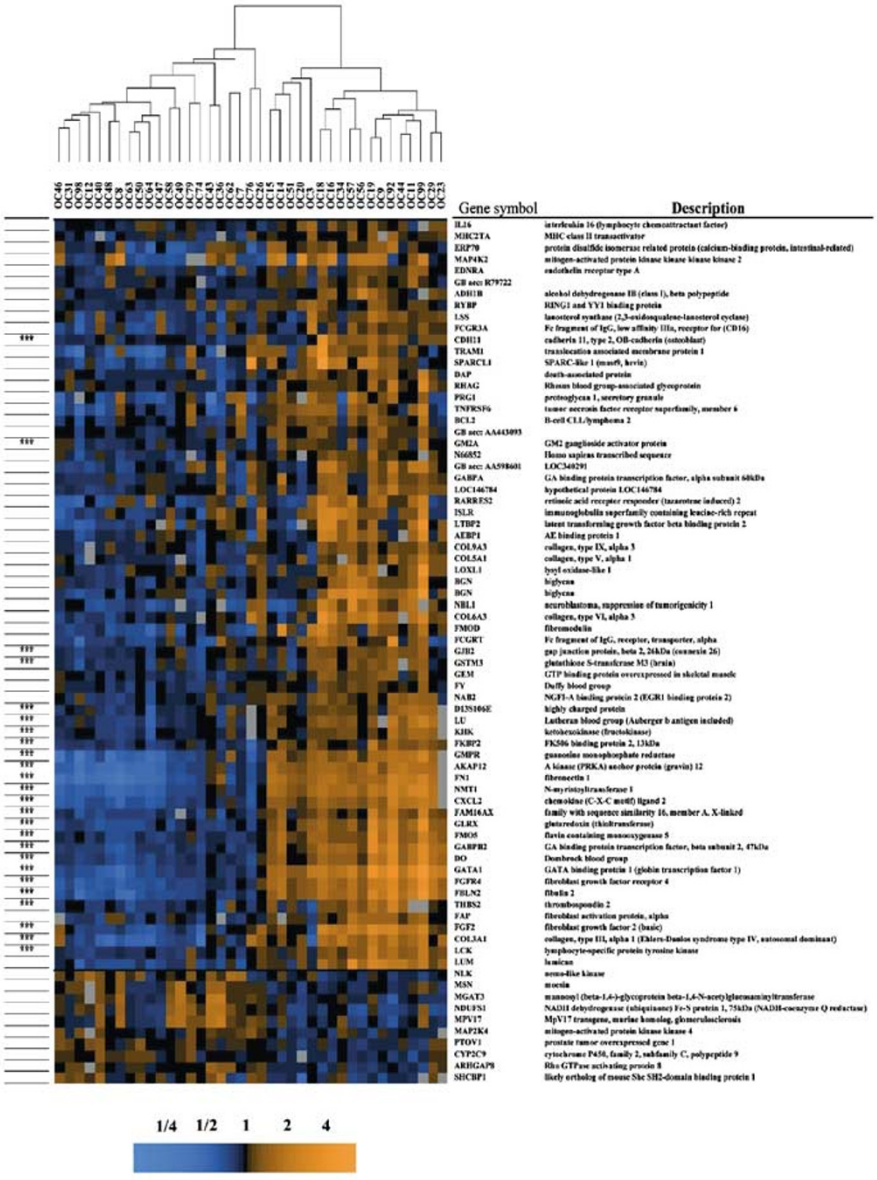

Figure 1 The ECM-FGF2 signaling molecular signature. Gene expression pattern determined by agglomerative hierarchical clustering of 39 primary ovarian cancer samples using the 75 clones extracted by ISIS. Expression levels are relative to a common reference, obtained by pooling RNA from 10 human cell lines. Increased (orange) or decreased (blue) expression of the genes is shown for each sample. Genes in common with the cellular-plasticity classifier are indicated on the left (see also Figure 4)

et al., 1994; Dyck *et al*., 1996; Kruk *et al*., 1994). We therefore investigated whether the *in vitro* phenotype displayed by ovarian cell lines was somehow related to the 'epithelial–mesenchymal plasticity' signature identified in EOC cells by the ISIS class discovery approach.

To extract the genes that best discriminate between the two cell line phenotypes, we applied a two-sample *t*-test (with randomized variance model and false discovery rate assessment in permutation test with a confidence interval of 90%). This analysis allowed the recovery of 113 clones (*P*-value in univariate *F*-test < 0.0025), 47 upregulated in epithelial-like cells and 66 upregulated in mesenchymal-like cells (Figure 4). The best fit was observed for cells with a well-defined epithelial or mesenchymal morphology. OSE cells at the first *in vitro* passage, in agreement with their intermediate phenotype, presented a less stringent association with the identified genes. In the OC67 sample, corresponding to the IOSE line and clustering with cells exhibiting mesenchymal morphology, some epithelial-associated genes were highlighted.

Interestingly, 25 of the 66 'mesenchymal phenotype'-associated genes were also present in the ECM gene list generated using the class discovery approach in EOC advanced tumor samples (see Figures 1 and 4). The common genes belonged to the largest functional category, including cell adhesion and cell–stroma inter-

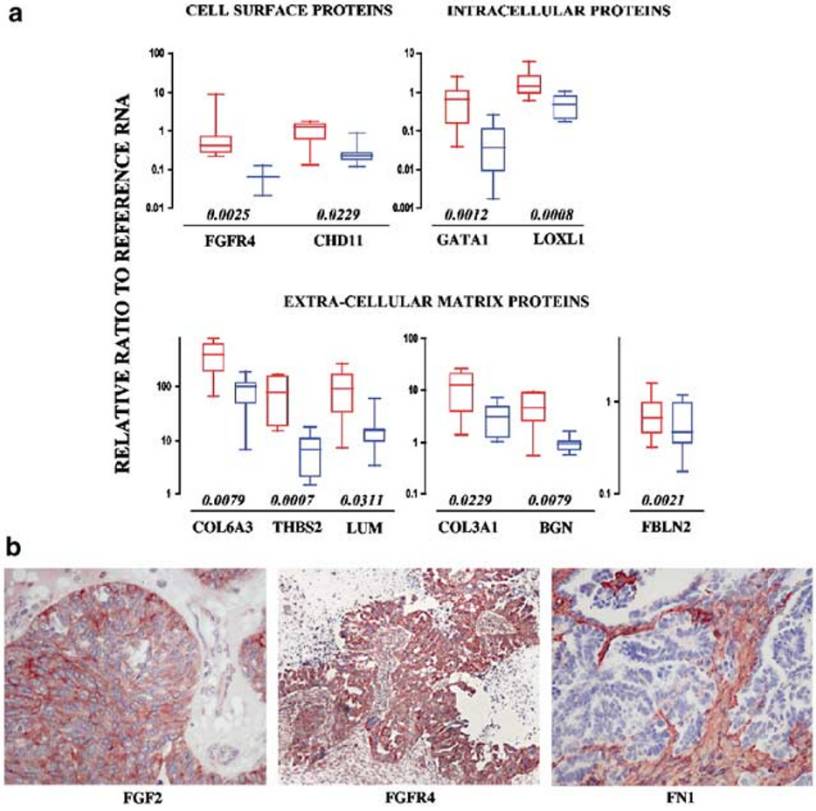

Figure 2 Validation of selected genes. **(a)** Expression patterns of 10 genes encoding cell surface (FGFR4 and CDH11), intracellular (GATA1 and LOXL1) and extracellular matrix (COL6A3, THBS2, LUM, COL3A1, BGN and FBLN2) proteins were examined in representative EOC samples displaying upregulation (red boxes, nine cases for all genes with the exception of FGFR4 for which only seven cases were available) and downregulation (blue boxes, nine cases for all genes with the exception of FGFR4 for which only five cases were available) of the ECM-related classifier genes. Each value was calculated as the ratio between the sample and the reference cDNA used to construct a standard curve. Results are expressed as boxed quartiles (median, 25th, and 75th percentile) and whiskers (minimum and maximum) statistically compared by Mann–Whitney test (*P*-values are reported for each comparison between expression levels in top-DLD-classifier up- or downregulated cases). (**b**) Immunohistochemistry validation of FGF2, FGFR4, and FN1 protein expression in EOC. A representative subset of either top-DLD-classifier up- or downregulated samples (12 and 10, respectively) was immunoreacted with specific antibodies. An example of each immunoreaction is shown. FGF2 and FN1, $\times 400$ original magnification; FGFR4, $\times 200$ original magnification

action (CDH11, FBLN2, THBS2, FN1, COL3A1) and cell signaling (FGF2, FGFR4). The differential expression of these genes was confirmed by TaqMan using independent RNA preparations from OC52, OC87, OC104, and OC67 (data not shown).

Together, these data suggested the feasibility of applying two independent approaches to identify a molecular signature common to some ovarian cell lines and to a subset of EOC related to plasticity processes of cancer cells.

In vitro *functional analysis of the identified molecular signature*

The availability of a pair of isogenic cell lines (h-TERT and IOSE) for the microarray profiling of cell lines enabled us to test operationally in a similar genetic background the significance of FGF2 signaling for cellular phenotype. FGF2 was chosen for the *in vitro* functional analysis due to its intrinsic manipulability. Real-time RT–PCR analysis of FGF2 gene expression confirmed the microarray data (Figure 5a and b). On a per-cell basis, ELISA revealed comparable levels of intracellular FGF2 in IOSE and h-TERT cell lysates, while a dramatic difference was observed in culture supernatants (Figure 5c). Indeed, $>90\%$ of total FGF2 was intracellular in h-TERT cells, while IOSE cells secreted high amounts of FGF2 into the culture supernatant. The release of FGF2 from IOSE cells was confirmed by ELISA using supernatants from a separate pair of isogenic IOSE/h-TERT cell lines (data not shown). Western blot analysis was performed on cell lysates and conditioned media to provide biochemical evidence of the FGF2 molecule (Figure 5d). The relative amounts of the different natural isoforms of FGF2 were comparable in cell lysates (lanes 1–2); on the contrary, the total amount and the different isoforms were different in conditioned media. The 24 and 18 kDa isoforms were clearly present in IOSE-conditioned medium (lane 3), while only a slight amount of 24 kDa isoform was detectable in h-TERT-conditioned medium (lane 4).

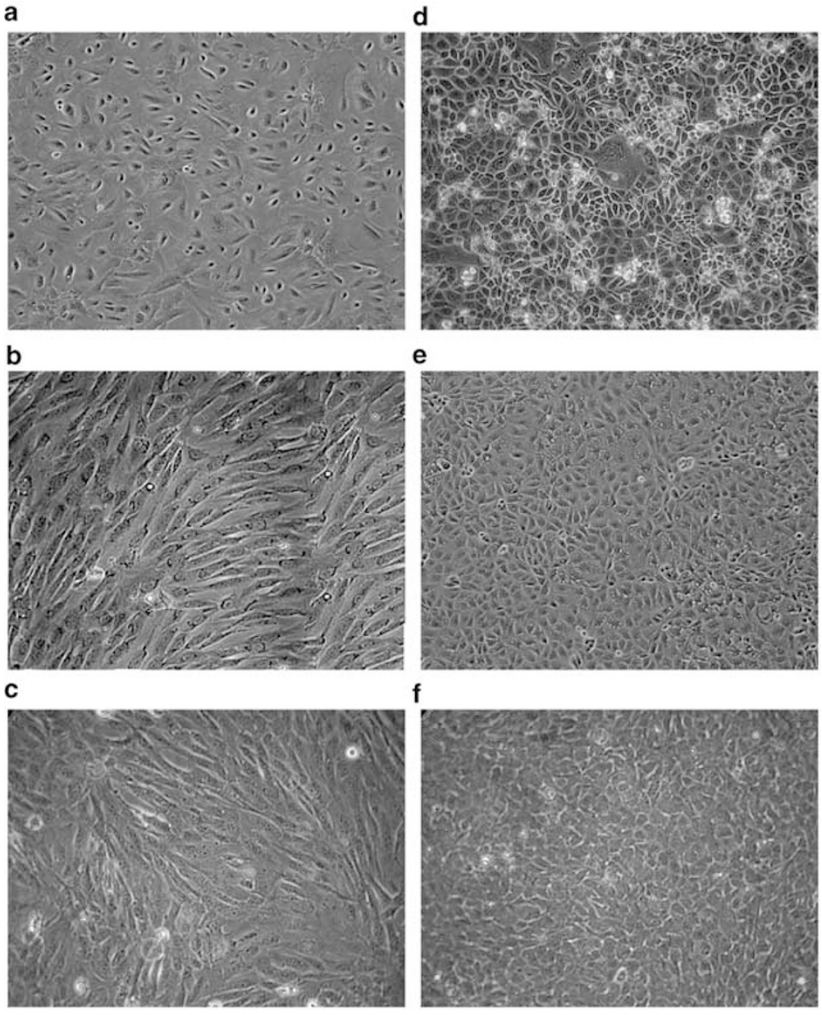

Figure 3 Morphology of cultured ovarian cells. Cells with mesenchymal-like morphology include: (**a**) OSE18/OC65 at the first *in vitro* passage; (**b**) OSE36/OC103 at the third *in vitro* passage; (**c**) IOSE/OC67. Cells with a typical epithelial or an epithelial-like morphology included: (**d**) IGROV1/OC52 ovarian cancer, (**e**) OAW42/OC87 ovarian cancer, (**f**) h-TERT/OC104 cells. × 100 original magnification in all panels

To further assess the role of secreted FGF2 on cell growth and migration, we analysed the ability of IOSE and h-TERT cells to migrate and scatter randomly in a wound repair assay (Figure 6a). Based on comparison of proliferation rates, wound closure rate was slower in IOSE than in h-TERT; however, the mesenchymal-like IOSE cells migrated individually in a scattered fashion into the wound, while the epithelial-like h-TERT cells repaired the wound without loss of cell–cell contacts. h-TERT cells in the presence of IOSE cell supernatants containing FGF2 tended to lose cell–cell contacts and to acquire a spindle-like morphology, seldom migrating as individual cells. FGF2-neutralizing antibodies inhibited cell proliferation and cohort/scattered migration in IOSE cells and in h-TERT cells cultured in the presence of IOSE cell supernatants. Hepatocyte growth factor (HGF)-neutralizing antibodies had no effect on proliferation or wound repair (shown only for IOSE cells in Figure 6a), consistent with the absence of HGF release by the cells (Turatti *et al*., manuscript in preparation), even when tested at 100-fold higher concentrations. Altogether these data advocate FGF2 as the responsible factor for the measured activity on h-TERT. To possibly identify the receptor responsible for FGF2 signaling, the FGFR expression of IOSE and h-TERT cells was evaluated by Western blot analysis of cell lysates. FGFR1 and 3 were absent or under the level of detectability of the assay (data not shown), while both FGFR2 and 4 were expressed in both cell lines (Figure 6b).

Together, these data suggest that FGF2 acts as an autocrine, but not intracrine, growth factor for OSE cells. In this context, FGF2 extracellular release stimulates proliferation in both epithelial- and mesenchimal-like types, sustains migration of cells with mesenchymal morphology, and induces scattering and morphological changes in cells with epithelial morphology. This latter phenomenon, also known as 'reversible scatter', is a well-documented phenocopy of the intermediate processes leading to the complete

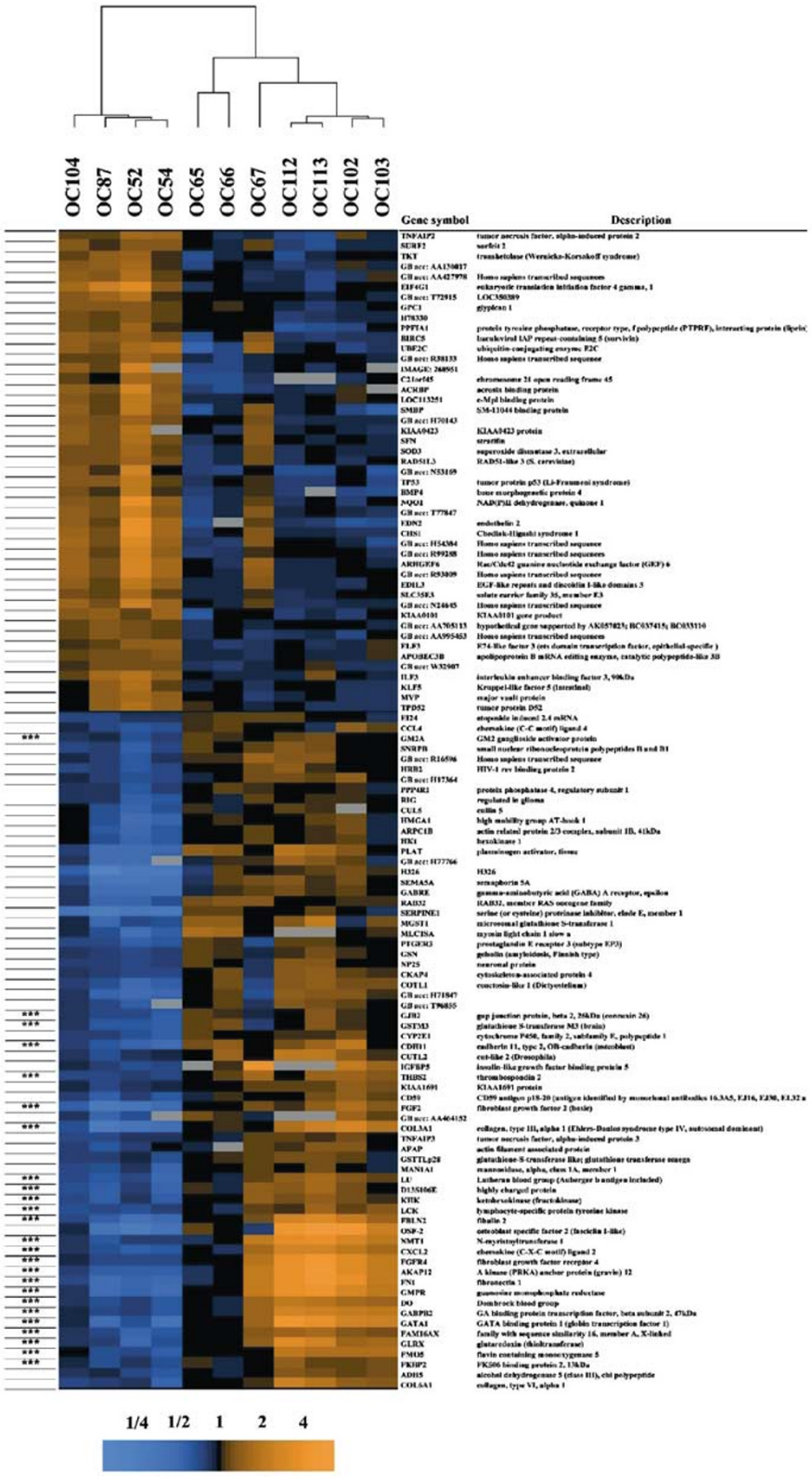

Figure 4 Clustering of cultured ovarian cells. Clustering was carried out based on the genes retrieved by class comparison. The genes retrieved were those that best discriminated between cell lines displaying mesenchymal or epithelial phenotypes (nominal *P*-value <0.0025 in two-sample univariate *F*-test with FDR correction). Expression levels are relative to a common reference, obtained by pooling RNA from 10 human cell lines. Increased (orange) or decreased (blue) expression of the genes is shown for each sample. Genes in common with the gene list associated with a subtype of EOC (see Figure 1) are indicated on the left

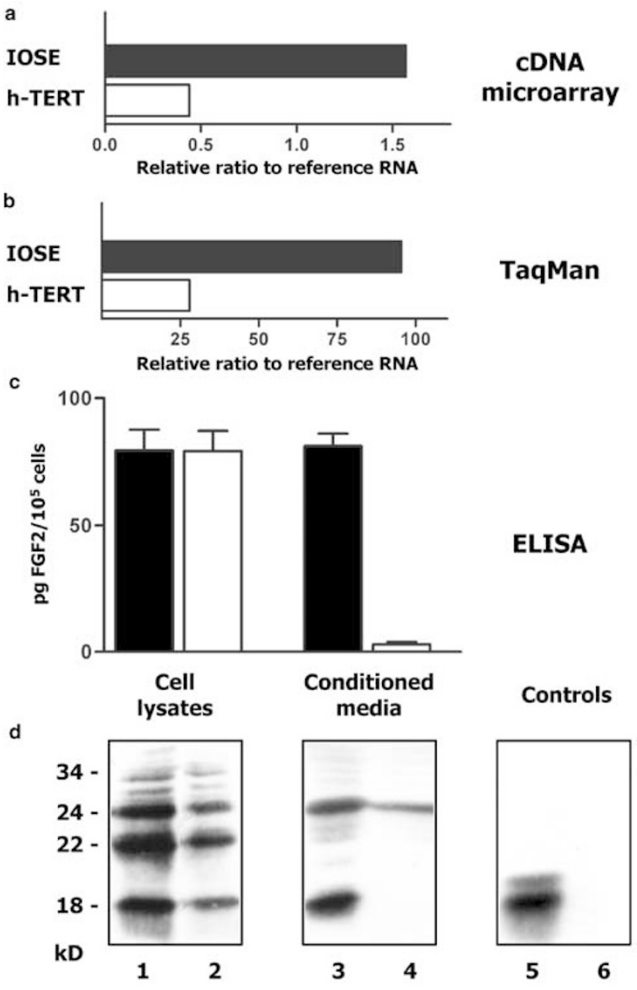

Figure 5 FGF2 production by IOSE (filled bars) and h-TERT (open bars) cells. (**a**) Relative FGF2 expression by cDNA microarray. (**b**) Relative FGF2 expression by real-time RT–PCR analysis. (**c**) Quantitation by ELISA of FGF2 in culture supernatants and cell lysates obtained from equivalent numbers of IOSE and h-TERT cells (mean $\pm$ s.d. of 5–6 independent experiments). (**d**) Expression of FGF2 as detected by Western blot analysis of cell lysates (lanes 1–2) and $10\times$-conditioned media (lanes 3–4) obtained by equivalent numbers of IOSE and h-TERT cells. As positive and negative controls $10\times$-concentrated medium containing (lane 5) or not containing (lane 6) recombinant FGF2 was used. See Figure 6b for loading control of cell lysates

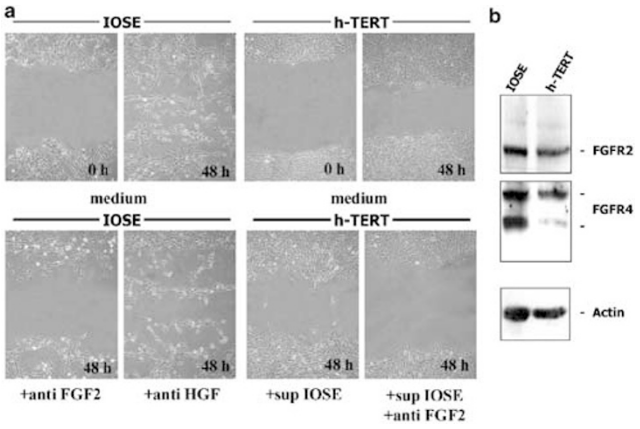

Figure 6 FGF2 signaling on IOSE and h-TERT cells. (**a**) Wound assay. IOSE and h-TERT cells at the time of scraping (0 h) and 48 h after wounding and culture in the presence of the indicated reagents (neutralizing anti-HGF and -FGF2 antibodies used at 5 and 0.05 μg/ml, respectively). Results are from one of six independent experiments with superimposable results. (**b**) FGFR2 and FGFR4 expression as detected by Western blot analysis of cell lysates. Actin was used as loading control

epithelial–mesenchymal transition, which occurs *in vitro* only after 4–6 days of exposure to triggering signals (Janda *et al*., 2002).

Discussion

In this study, we analysed gene expression profiles obtained in a large set of samples of ovarian origin, including several cell lines and a well-defined tumor set from a single-center tumor bank coupled with patient data. Our findings identify a previously unknown subset of EOC, characterized by a specific molecular signature related to OSE cell plasticity.

Using our cDNA microarray dataset, we analysed stages III–IV EOC by an unsupervised class discovery approach (ISIS), which identified binary partitions of tumor samples. Analysis of the associated gene lists delineated a distinct profile of gene expression enriched in several genes encoding ECM components and accounting for genes involved in FGF2 signaling. Involvement of several of these genes was validated by quantitative RT–PCR and immunohistochemical staining on representative tumors samples, consistent with the cDNA microarray measurements. Supervised learning (class comparison) was applied to ovarian-derived cell lines exhibiting distinct morphology in culture, leading to the discovery of a gene classifier related to cellular plasticity (epithelial- versus mesenchymal-like morphology). Notably, about 40% of genes associated with the ECM/FGF2 signaling-related ISIS class overlapped with the genes upregulated in mesenchymal-like cells and were partially similar to the 'extracellular matrix stromal' cluster previously described (Schaner *et al*., 2003). However, the simple interpretation that the identified ECM molecular signature corresponds to the stromal content of the specimens seems unlikely since all of our samples presented a tumor cellularity greater than 70% and a similar signature was identified using *in vitro* cultures of pure OSE cells.

The lack of correlation between the genes associated with the epithelial morphology of cancer cell lines and the gene list identified with tumor samples might rest, in part, in the intrinsic limitation of *in vitro* cultures and in the peculiar features of ovarian surface epithelium. On the one hand, cancer cells stably adapted to growth *in vitro* tend to lose their dependence on microenvironmental signals, so that their gene expression might only partially reflect the *in vivo* situation. On the other hand, normal OSE cells display both epithelial and

mesenchymal characteristics and retain a high degree of plasticity, enabling them to alter their state along the mesenchymal or epithelial differentiation programs in a highly dynamic manner. This feature is partially maintained at the first passage in culture and can be modulated by different external signals (Auersperg *et al*., 1994; Dyck *et al*., 1996; Kruk *et al*., 1994).

The list of genes identified accounted for a large number of structural components of ECM and its remodeling, and for proteins involved in FGF2 signaling, cell adhesion, and cell-to-cell signaling processes. Several genes in these categories have already been associated with ovarian and/or other cancer progression, for example, increased in COL3A1 production, along with COL1A1, has been observed in advanced ovarian cancers and shown to be a prognostic marker of poor outcome (Simojoki *et al*., 2001; Santala *et al*., 1999), while COL6A3 and several ECM genes are reported to be highly upregulated in cisplatin-resistant cells (Sherman-Baust *et al*., 2003), and THBS1 and THBS2 expression has recently been associated with advanced ovarian cancer, suggesting a role for these molecules in the progression of this type of malignancy (Kodama *et al*., 2001).

The gene list defined herein also included several members of the FGF2 signaling pathway, which are known to be expressed in ovarian and EOC cells (Crickard *et al*., 1994; Di Blasio *et al*., 1995; Valve *et al*., 2000), and several other genes regulated by FGF2 in various contexts: CDH11 is specifically regulated by FGF2 in models of kidney fibrosis (Strutz *et al*., 2002), LUM expression is induced by FGF2 in keratocytes of the corneal stroma (Long *et al*., 2000), while BGN is similarly controlled in aortic endothelial cells (Kinsella *et al*., 1997). Coexpression of the latter molecules could also be related to the evidence that FGF family members bind to heparan sulfate proteoglycans of the ECM, with such interaction comprising part of the regulation of the FGF signaling unit (Plotnikov *et al*., 1999; Plotnikov *et al*., 2000; Schlessinger *et al*., 2000). Moreover, we identified GATA1 among the genes coexpressed with FGF2/FGFR4 in both the EOC subset and the analysed cell lines, suggesting that GATA factors act as downstream effectors of the FGF signaling. Indeed, at least one member of the GATA family (aGATA) was recently shown to act downstream of FGF signaling in ascidians to determine induction of a neuronal fate in animal cells (Bertrand *et al*., 2003).

The role of the FGF2 signaling in the pathogenesis and progression of EOC remains controversial. Some authors have proposed that FGF2 and other members of the FGF family contribute to growth, invasion, and metastasis by neovascularization (Fujimoto *et al*., 1997), while others have suggested that FGF2 induces a fibroblastic response capable of reducing aggressiveness of tumors through high FGF2 expression levels (Obermair *et al*., 1998). The lack of association between expression of ECM/FGF2 signaling-related classifier and overall survival observed in our study might reflect a more complex *in vivo* regulation of the FGF2 signaling and the involvement of additional factors in the tumor progression of the two groups of patients. Moreover, this molecular signature is already evident in the very initial steps of carcinogenesis, as demonstrated not only in the OSE cells but also in the few borderline and early FIGO stage tumors in our collection (data not shown). Within this framework, the molecular signature we discovered might indicate an altered interaction between plastic tumor cells and the surrounding stroma. The relevance of the identified molecular signature is strongly suggested, even when the physiologic or pathologic crosstalk between the different tissue components of the ovary is taken into account. As recently outlined (Liotta and Kohn, 2002), a homeostatic feedback circuit between normal OSE and the underlying stroma precludes the implant of desquamated normal cells, while neoplastic ovarian cancer cells may positively respond to or even actively recruit stromal cells (Parrott *et al*., 2001) and induce stroma-derived molecular signals.

FGF receptors bind members of the FGF family with varying affinity, but the biological consequences of binding are not merely function of affinity, being also related to the cellular and physiological context, as linked to the expression of coreceptor molecules such as proteoglycans which critically contribute to the ligand-receptor specificity and signal-transduction ability (Plotnikov *et al*., 1999; Schlessinger *et al*., 2000). Furthermore, alternative mRNA splicing leads to isoforms of FGFR that have unique ligand-binding properties (Powers *et al*., 2000). Taking into account our data and the detailed studies in ovarian cancer (Steele *et al*., 2001; Valve *et al*., 2000), we could focus on either FGFR2 or FGFR4 as possible candidates for FGF2 specific signaling. Owing to the reported complexity of FGFs/FGFRs expression and the relevance of the cellular context in their interaction, further studies are needed to define the relative contribution of the two receptors, and to know which isoform of FGFR2 is relevant in FGF2 signaling on normal and tumor cells.

To contextualize the role of the identified molecular signature in the framework of EOC pathogenesis and progression, we focused on FGF2 signaling for further *in vitro* biological evaluation. Our results using two independent pairs of isogenic cell lines displaying opposite expression of the identified classifier demonstrated that FGF2 is released into the extracellular space (Figure5 and data not shown) only by mesenchymal classifier-positive cells and not by epithelial classifier-negative cells. However, both IOSE and h-TERT cell lines, in the wound repair assay, responded with increased migration to FGF2 present in the medium, and the epithelial cell line showed 'reversible scatter', a necessary intermediate step toward a complete mesenchymal conversion *in vitro* (Janda *et al*., 2002). FGF2 lacks signal peptide but yet could be exported to the extracellular space, and, accordingly, it is considered as an unconventionally secreted protein. Recent reports provide experimental evidence for FGF2 release through vesicle shedding (Taverna *et al*., 2003) or direct translocation across the plasma membrane (Schafer

et al., 2004) and work is in progress to identify the mechanism utilized by OSE/IOSE cells for FGF2 export.

The central role of FGF signaling is underlined not only by the results of our *in vitro* experiments but also by the large body of literature underscoring the multiple and pleiotropic effect of this conserved signaling pathway (Powers *et al*., 2000; Ornitz and Marie, 2002; Thiery 2002). The FGF family of signaling molecules contributes to normal development and various physiological processes, such as neural and mesenchymal commitment/differentiation through an autocrine/paracrine loop with their receptors, indicating a prominent role for this signaling pathway in maintaining cellular plasticity (Bertrand *et al*., 2003; Sheng *et al*., 2003). In addition, accumulated evidence in various pathological conditions has indicated a dual role for FGF2 signaling in triggering different processes, such as epithelial-to-mesenchymal and mesenchymal-to-epithelial transitions (Karavanova *et al*., 1996; Perantoni *et al*., 1995). Overall, these data show that interpretation of FGF2 signaling only in terms of the epithelial-to-mesenchymal transition is equivocal and does not account for the complexity of cellular plasticity processes, which are especially relevant in EOC pathogenesis.

An unusual aspect of ovarian carcinogenesis is the change in differentiation that accompanies neoplastic progression, wherein cancer cells acquire the characteristics of Mullerian duct-derived epithelia. This aberrant differentiation occurs in a high proportion of ovarian carcinomas that it represents the basis for the classification of EOC (Auersperg *et al*., 2001). Thus, unlike cancers arising in other organs where epithelial cells become less differentiated during progression, a process of epithelial differentiation, coupled with expression of several epithelial markers, accompanies the EOC pathogenesis and progression (Van Niekerk *et al*., 1993; Darai *et al*., 1997; Maines-Bandiera and Auersperg, 1997; Sundfeldt *et al*., 1997; Davies *et al*., 1998). Our observations indicate the existence of a mesenchymal signature in a subset of advanced EOC, possibly sustained by an autocrine FGF2/FGFRs loop. In this subset, the original epithelial plasticity of the tissue of origin appears to be maintained, although with Mullerian differentiation characteristics. The FGF2 signaling genes revealed by our analysis might be key players in the maintenance of ovarian cancer cell plasticity, and their roles in EOC might extend to the control of epithelial–mesenchymal interactions rather than the simple induction of epithelial-to mesenchymal transition in this tissue.

Our observed lack of association between the expression of the identified classifier and overall survival could indicate a complex *in vivo* regulation of the FGF2/FGFR signaling and the genes associated with the classifier in ovarian carcinoma. In this scenario, accumulated evidence has indicated that a complex modulation network exists at the level of FGFRs signaling functions, where a number of cell adhesion molecules have been shown to modulate their signaling (Walsh and Doherty, 1997). Studies are in progress to evaluate if the combination of adhesion molecule expression with an FGF/ECM-classifier positive profiling could result in significant predictive values.

These findings might provide the basis for the rational design of effective therapeutic modalities focused on aspects of ovarian cancer cell plasticity.

Materials and methods

Samples

All clinical specimens used in this study were obtained with Institutional Review Board approval from 47 previously untreated patients with histologically confirmed EOC (stages I–IV according to FIGO criteria) and from three patients with benign (one woman) or borderline (two women) tumors who underwent exploratory laparatomy at the Istituto Nazionale Tumori, Milan, between 1990 and 2000. Informed consent to use leftover biological material for investigation purposes was obtained from all patients participating in the study. Tissue samples were taken at the time of initial surgery, immediately frozen in liquid nitrogen and stored at $-80^{\circ}C$ until used. All tumor samples were evaluated by a pathologist, and regions containing tumor cellularity greater than 70% were sharp-dissected and homogenized. Clinical information was available for each tumor sample and is summarized in Table 1. In five cases, ascitic fluids were obtained, cells recovered and characterized for tumor marker expression (Supplementary section d). In 42 cases, solid tumors were screened for the presence of TP53 mutations in the most frequently affected exons (5–8) of the gene (Supplementary section e).

The majority of tumors were classified as stages III–IV and grade 3. Borderline and stage I patients received only surgical resection, while stages III–IV patients after surgical debulking received conventional first-line chemotherapy containing taxanes and platinum compounds. The residual disease after debulking was recorded for all patients, and overall survival was calculated from the time of the first surgery. Patients were considered resistant to front-line chemotherapy if the disease progressed on treatment or was reduced by less than 50% within 6 months from the initial surgery. These patients and all others who relapsed later on received further chemotherapy.

The following human ovarian cells in culture were used: serous carcinoma lines IGROV1 (a gift from J Bénard, Institute Gustave Roussy, Villejuif, France) (OC52) and its cisplatinum-resistant sublines IGROV1/Pt0.1 (OC54) (Righetti *et al*., 1999) and OAW42 (OC87) (DKFZ, Heidelberg, Germany); five short-term cultures of OSE cells; simian virus 40 (SV40) large T antigen-immortalized IOSE11 (OC112), used at culture passage 10; SV40-immortalized IOSE-80 (hereafter designated IOSE) (OC67) (kindly provided by Dr N Auersperg, University of British Columbia, Vancouver, British Columbia, Canada); and IOSE-h-TERT (hereafter designated h-TERT) (OC104), obtained by stable transfection of IOSE cells with h-TERT cDNA (kindly provided by Dr RA Weinberg, Whitehead Institute, Cambridge, MA, USA). OSE cells were scraped from the surface of normal ovaries obtained at surgery for benign or malignant gynecological diseases other than ovarian carcinoma and maintained in culture for one (OC65, OC66) or three (OC102, OC103, OC113) passages as described (Kruk *et al*., 1990).

A total of 10 human cell lines of different origins were used to prepare the reference RNA for microarray analyses: U2OS osteosarcoma; SKNMC medulloblastoma; HeLa and C33A cervical carcinomas; A2780 mucinous ovarian carcinoma;

HT29 colon carcinoma; MDA231 mammary carcinoma; DUI45 prostate carcinoma; KG1A lymphoma; and LT2 endothelial cells. All cell lines were obtained from and maintained as instructed by American Type Culture Collection (ATCC).

cDNA microarrays

The cDNA microarrays used in this study contain 4451 unique clones selected from the Human sequence-verified I.M.A.G.E. clone collection (Research Genetics/Invitrogen). Additional cDNA clones selected from our proprietary cDNA libraries were added as internal controls, along with plant genes, printing controls (water/DMSO), and spike genes (Amersham Biosciences, Amersham, UK). The list of annotated genes is available from the web sites of IFOM (http://www.ifom.it/) and LNCIB (http://www.lncib.it/).

The cDNA fragments were PCR-amplified, reaction products were purified with Multiscreen PCR 96-well filtration system (Millipore, Bedford, MA, USA) and spotted in triplicate on type 7 star slides (Amersham Biosciences, Amersham, UK), using a Microarray Spotter Generation III (Amersham Biosciences) and ASC-XT high-density software (Amersham Biosciences) **(**Supplementary section f).

RNA isolation and cDNA microarray techniques

Total RNA was extracted using Trizol (Life Technologies, Frederick, MD, USA) following the manufacturer's instructions. Integrity of the RNA was assessed by agarose gel electrophoresis after DNase I and clean-up treatment with RNaesy mini kit (Qiagen, Valencia, CA, USA). All tumors specimens processed contained at least 70% of cancer cells. A radiolabeled tracer was added during the cDNA synthesis and a small amount of the cDNA was run on an alkaline gel (1% agarose, 50 mM NaOH, 1 mM EDTA). Only cDNAs showing a similar core size of 1–1.5 k nucleotides were used for subsequent hybridization. The target cDNAs were synthesized from total RNA and labeled directly with Cy3-dCTP (reference RNA) or Cy5-dCTP (sample RNA) (Amersham Biosciences) and indirectly with 3DNA Submicro Expression Array Detection kit (Genisphere, Montvale, NJ, USA). Total RNA was reverse transcribed using 5′ end modified oligo-dT primers containing the specific Cy3 or Cy5 3DNA capture sequences. The ^{32}P-labeled cDNAs with an estimated activity of about 100 000 c.p.m. were annealed with 1.5 μl of the specific 3DNA capture reagent for 16 h at 41°C. Hybridization was carried out in a hybridization station (Genomic Solutions, Ann Arbor, MI, USA) and slides were scanned using the GenePix 4000A microarray scanner (Axon Instruments, Union City, CA, USA) (Supplementary sections g–i).

Data analysis

Dataset filtering and normalization (mean centering) were performed using J-Express (Molmine) (Dysvik and Jonassen, 2001). Automated unsupervised class discovery was performed using the ISIS software v.2.0 (von Heydebreck *et al*., 2001). Hierarchical clustering analysis and class comparison analysis were performed using BRB ArrayTools (developed by Dr Richard Simon and Amy Peng, Biometric Research Branch, Division of Cancer Treatment and Diagnosis, National Cancer Institute; http://linus.nci.nih.gov/BRB-ArrayTools.html) (McShane *et al*., 2002; Radmacher *et al*., 2002). Briefly, ISIS software was used to identify candidate binary partitions of the tumor samples, while a two-sample univariate *F*-test (with randomized variance model and false discovery rate assessment) was applied to extract the list of associated genes, which is not obtained as an output of the ISIS procedure (Supplementary sections b and c). A two-sample *T*-test was also used to extract the best discriminating genes between distinct classes of samples on the basis of known phenotypes (e.g. between cell lines displaying distinct cellular phenotypes); false discovery rate was assessed in a permutation test with a 90% confidence interval. A maximum of 10 false-positive genes and a maximum proportion of 0.1 false-positive genes were allowed. GO terms analysis was carried out using EASE software v. 2.0 (available at http://david.niaid.nih.gov/david/) by comparing the GO-terms distribution of gene lists extracted using the two-sample *t*-test with the GO-terms distribution of the valid genes of our cDNA microarray. *P*-values obtained in Fisher's exact test and the EASE score were corrected using several alternative methods (Bonferroni, Sidak, Hochberg, Benjamini, Bootstrap iteration) (Hosack *et al*., 2003) (see Supplementary section b and j).

Quantitative RT–PCR

Total RNA used for microarray experiments (for cell lines, independent RNA preparationswere used) was reverse-transcribed using the High-Capacity cDNA Archive Kit. TaqMan TM reactions were carried out in duplicate on an ABI PRISM 7700 machine, using Assays-on-Demand Gene Expression Products (Applied Biosystems, Foster City, CA, USA). Data analysis was performed using the Sequence Detector v1.7 software, and statistical evaluations were performed using GraphPad software (GraphPad Software Inc., San Diego, CA, USA).

Immunohistochemical staining

Immunohistochemistry assays were performed using routine tissue blocks. Conditions of antigen retrieval and dilutions were optimized for each of the following antibodies: anti-FGF2 and anti-FGFR4 (Santa Cruz), anti-FN1 (Dako). After three washes in PBS-1% Triton, slides were incubated with secondary antibody (goat anti-rabbit or rabbit anti-goat biotinylated IgG diluted 1 : 100 and 1 : 50, respectively, in PBS-1% BSA-0.1% sodium azide; DAKO) for 30 min at room temperature. Negative controls included sections incubated with an appropriate blocking peptide or with nonimmune serum of the respective species instead of primary antibody. After final incubation with streptavidin-conjugated horseradish peroxidase (DAKO) (diluted 1 : 300 in PBS) for 30 min at room temperature and after several washings in PBS-0.1% Triton, peroxidase acivity was detected by aminoethyl carbazole for 10 min in the dark. Slides were counterstained with Carazzi hematoxylin (Supplementary section k).

FGF2 production and biological activity assays

IOSE and h-TERT cells were seeded in six-well plates containing 1 ml of medium. Culture supernatants were harvested when cells reached confluence, and cells were counted and lysed. FGF2 levels were assayed in culture supernatants and cell lysates using the Quantikine human FGF2 immunoassay (R&D Systems, Minneapolis, MN, USA). For wounding assay of scatter/cohort migration, semiconfluent cells in standard medium were gently scraped with a rubber policeman, the medium harvested, cleared of debris and replaced in the presence or absence of 5 or 0.05 μg/ml neutralizing antibodies directed against h-HGF (R&D Systems) and h-FGF2 (Calbiochem, La Jolla, CA, USA) (Hori *et al*., 1991), respectively. The effect of released FGF2 on h-TERT cells was evaluated using freshly collected culture supernatants from confluent IOSE cells. In all cases, cells were

allowed to scatter/migrate into the cleared area for 48 h. For Western blot analysis, IOSE or h-TERT cells at confluence were washed twice in cold PBS and lysed for 15 min on ice in lysis buffer (10 mM Tris pH 7.5, 150 mM NaCl, 1 mM EDTA, 0.02% NaN_3, 1% NP40 0.1% SDS). Lysates or $10\times$-concentrated conditioned media were separated by 7.5 and 15% SDS–PAGE, respectively, for FGFR and FGF2 detection and transferred to a nitrocellulose membrane (Hybond C-Super, Amersham). Immunoreaction was carried out using the anti FGFR1-4 primary antibodies from Santa Cruz and the neutralizing anti-FGF2 Mab following the suggested procedures and was visualized with the enhanced chemiluminescence technique (ECL; Amersham).

Statistical analysis

Differences between the expression pattern of selected genes validated by quantitative RT–PCR were assessed by the Mann–Whitney U-test. Kaplan–Meyer curves were used to estimate patient survival (defined as the time, in months, from initial surgery until death) among each subset of stages III–IV EOC patients. The log-rank test was used to assess differences between survival curves. All *P*-values were two-sided. Statistical analyses were performed using SAS (SAS Institute, Cary, NC, USA) and GraphPad (GraphPad Software Inc., San Diego, CA, USA) software.

Acknowledgements

Support for this project was provided to INT (Istituto Nazionale Tumori) – LNCIB (Laboratorio Nazionale CIB) by AIRC (Associazione Italiana Ricerca sul Cancro) Coordinated Project at IFOM (FIRC Institute for Molecular oncology) 'Detection of cancer gene mutation and expression profiling by nanotechnology' and by CNR/MIUR 'Progetto strategico Oncologia' (contract no. 02.00385.ST97 to MA Pierotti and no. 02.00386.ST97 to C Schneider) and grants to S Canevari from AIRC-FIRC and Special Project of Health Ministry.

References

Auersperg N, Maines-Bandiera SL, Dyck HG and Kruk PA. (1994). *Lab. Invest.*, **71,** 510–518.

Auersperg N, Wong AS, Choi KC, Kang SK and Leung PC. (2001). *Endocr. Rev.*, **22,** 255–288.

Aunoble B, Sanches R, Didier E and Bignon YJ. (2000). *Int. J. Oncol.*, **16,** 567–576.

Balli S, Fey MF, Hanggi W, Zwahlen D, Berclaz G, Dreher E and Aebi S. (2000). *Eur. J. Cancer*, **36,** 2061–2068.

Bertrand V, Hudson C, Caillol D, Popovici C and Lemaire P. (2003). *Cell*, **115,** 615–627.

Crickard K, Gross JL, Crickard U, Yoonessi M, Lele S, Herblin WF and Eidsvoog K. (1994). *Gynecol. Oncol.*, **55,** 277–284.

Darai E, Scoazec JY, Walker-Combrouze F, Mlika-Cabanne N, Feldmann G, Madelenat P and Potet F. (1997). *Hum. Pathol.*, **28,** 922–928.

Davies BR, Worsley SD and Ponder BA. (1998). *Histopathology*, **32,** 69–80.

Di Blasio AM, Carniti C, Vigano P and Vignali M. (1995). *J. Steroid. Biochem. Mol. Biol.*, **53,** 375–379.

Dyck HG, Hamilton TC, Godwin AK, Lynch HT, Maines-Bandiera SL and Auersperg N. (1996). *Int. J. Cancer*, **69,** 429–436.

Dysvik B and Jonassen I. (2001). *Bioinformatics*, **17,** 369–370.

Feeley KM and Wells M. (2001). *Histopathology*, **38,** 87–95.

Fujimoto J, Ichigo S, Hori M, Hirose R, Sakaguchi H and Tamaya T. (1997). *Eur. J. Gynaecol. Oncol.*, **18,** 349–352.

Greenlee RT, Hill-Harmon MB, Murray T and Thun M. (2001). *CA Cancer J. Clin.*, **51,** 15–36.

Holschneider CH and Berek JS. (2000). *Semin. Surg. Oncol.*, **19,** 3–10.

Hori A, Sasada R, Matsutani E, Naito K, Sakura Y, Fujita T and Kozai Y. (1991). *Cancer Res.*, **51,** 6180–6184.

Hosack DA, Dennis Jr G, Sherman BT, Lane HC and Lempicki RA. (2003). *Genome Biol.*, **4,** R70.

Hough CD, Cho KR, Zonderman AB, Schwartz DR and Morin PJ. (2001). *Cancer Res.*, **61,** 3869–3876.

Hough CD, Sherman-Baust CA, Pizer ES, Montz FJ, Im DD, Rosenshein NB, Cho KR, Riggins GJ and Morin PJ. (2000). *Cancer Res.*, **60,** 6281–6287.

Janda E, Lehmann K, Killisch I, Jechlinger M, Herzig M, Downward J, Beug H and Grunert S. (2002). *J. Cell Biol.*, **156,** 299–313.

Jazaeri AA, Yee CJ, Sotiriou C, Brantley KR, Boyd J and Liu ET. (2002). *J. Natl. Cancer Inst.*, **94,** 990–1000.

Karavanova ID, Dove LF, Resau JH and Perantoni AO. (1996). *Development*, **122,** 4159–4167.

Kinsella MG, Tsoi CK, Jarvelainen HT and Wight TN. (1997). *J. Biol. Chem.*, **272,** 318–325.

Kodama J, Hashimoto I, Seki N, Hongo A, Yoshinouchi M, Okuda H and Kudo T. (2001). *Anticancer Res.*, **21,** 2983–2987.

Kruk PA, Maines-Bandiera SL and Auersperg N. (1990). *Lab. Invest.*, **63,** 132–136.

Kruk PA, Uitto VJ, Firth JD, Dedhar S and Auersperg N. (1994). *Exp. Cell Res.*, **215,** 97–108.

Liotta LA and Kohn EC. (2002). *J. Natl. Cancer Inst.*, **94,** 1113–1114.

Long CJ, Roth MR, Tasheva ES, Funderburgh M, Smit R, Conrad GW and Funderburgh JL. (2000). *J. Biol. Chem.*, **275,** 13918–13923.

Maines-Bandiera SL and Auersperg N. (1997). *Int. J. Gynecol. Pathol.*, **16,** 250–255.

Matei D, Graeber TG, Baldwin RL, Karlan BY, Rao J and Chang DD. (2002). *Oncogene*, **21,** 6289–6298.

Matias-Guiu X and Prat J. (1998). *Virchows Arch.*, **433,** 103–111.

McShane LM, Radmacher MD, Freidlin B, Yu R, Li MC and Simon R. (2002). *Bioinformatics*, **18,** 1462–1469.

Murdoch AD, Dodge GR, Cohen I, Tuan RS and Iozzo RV. (1992). *J. Biol. Chem.*, **267,** 8544–8557.

Obermair A, Speiser P, Reisenberger K, Ullrich R, Czerwenka K, Kaider A, Zeillinger R and Miksche M. (1998). *Cancer Lett.*, **130,** 69–76.

Ornitz DM and Marie PJ. (2002). *Genes Dev.*, **16,** 1446–1465.

Parrott JA, Nilsson E, Mosher R, Magrane G, Albertson D, Pinkel D, Gray JW and Skinner MK. (2001). *Mol. Cell. Endocrinol.*, **175,** 29–39.

Perantoni AO, Dove LF and Karavanova I. (1995). *Proc. Natl. Acad. Sci. USA*, **92,** 4696–4700.

Plotnikov AN, Hubbard SR, Schlessinger J and Mohammadi M. (2000). *Cell*, **101,** 413–424.

Plotnikov AN, Schlessinger J, Hubbard SR and Mohammadi M. (1999). *Cell*, **98,** 641–650.

Powers CJ, McLeskey SW and Wellstein A. (2000). *Endocr. Relat. Cancer*, **7,** 165–197.

Radmacher MD, McShane LM and Simon R. (2002). *J. Comput. Biol.*, **9,** 505–511.
Righetti SC, Perego P, Corna E, Pierotti MA and Zunino F. (1999). *Cell Growth Differ.*, **10,** 473–478.
Santala M, Simojoki M, Risteli J, Risteli L and Kauppila A. (1999). *Clin. Cancer Res.*, **5,** 4091–4096.
Schafer T, Zentgraf H, Zehe C, Brugger B, Bernhagen J and Nickel W. (2004). *J. Biol. Chem.*, **279,** 6244–6251.
Schaner ME, Ross DT, Ciaravino G, Sorlie T, Troyanskaya O, Diehn M, Wang YC, Duran GE, Sikic TL, Caldeira S, Skomedal H, Tu IP, Hernandez-Boussard T, Johnson SW, O'Dwyer PJ, Fero MJ, Kristensen GB, Borresen-Dale AL, Hastie T, Tibshirani R, van de RM, Teng NN, Longacre TA, Botstein D, Brown PO and Sikic BI. (2003). *Mol. Biol. Cell*, **14,** 4376–4386.
Schlessinger J, Plotnikov AN, Ibrahimi OA, Eliseenkova AV, Yeh BK, Yayon A, Linhardt RJ and Mohammadi M. (2000). *Mol. Cell*, **6,** 743–750.
Schwartz DR, Kardia SL, Shedden KA, Kuick R, Michailidis G, Taylor JM, Misek DE, Wu R, Zhai Y, Darrah DM, Reed H, Ellenson LH, Giordano TJ, Fearon ER, Hanash SM and Cho KR. (2002). *Cancer Res.*, **62,** 4722–4729.
Schwartz DR, Wu R, Kardia SL, Levin AM, Huang CC, Shedden KA, Kuick R, Misek DE, Hanash SM, Taylor JM, Reed H, Hendrix N, Zhai Y, Fearon ER and Cho KR. (2003). *Cancer Res.*, **63,** 2913–2922.
Sheng G, dos RM and Stern CD. (2003). *Cell*, **115,** 603–613.
Sherman-Baust CA, Weeraratna AT, Rangel LB, Pizer ES, Cho KR, Schwartz DR, Shock T and Morin PJ. (2003). *Cancer Cell*, **3,** 377–386.
Shridhar V, Lee J, Pandita A, Iturria S, Avula R, Staub J, Morrissey M, Calhoun E, Sen A, Kalli K, Keeney G, Roche P, Cliby W, Lu K, Schmandt R, Mills GB, Bast RCJ, James CD, Couch FJ, Hartmann LC, Lillie J and Smith DI. (2001). *Cancer Res.*, **61,** 5895–5904.
Simojoki M, Santala M, Risteli J and Kauppila A. (2001). *Gynecol. Oncol.*, **82,** 110–115.
Steele IA, Edmondson RJ, Bulmer JN, Bolger BS, Leung HY and Davies BR. (2001). *Oncogene*, **20,** 5878–5887.
Strutz F, Zeisberg M, Ziyadeh FN, Yang CQ, Kalluri R, Muller GA and Neilson EG. (2002). *Kidney Int.*, **61,** 1714–1728.
Sundfeldt K, Piontkewitz Y, Ivarsson K, Nilsson O, Hellberg P, Brännström M, Janson PO, Enerbäck S and Hedin L. (1997). *Int. J. Cancer*, **74,** 275–280.
Taverna S, Ghersi G, Ginestra A, Rigogliuso S, Pecorella S, Alaimo G, Saladino F, Dolo V, Dell'Era P, Pavan A, Pizzolanti G, Mignatti P, Presta M and Vittorelli ML. (2003). *J. Biol. Chem.*, **278,** 51911–51919.
Thiery JP. (2002). *Nat. Rev. Cancer*, **2,** 442–454.
Tonin PN, Hudson TJ, Rodier F, Bossolasco M, Lee PD, Novak J, Manderson EN, Provencher D and Mes-Masson AM. (2001). *Oncogene*, **20,** 6617–6626.
Tsao SW, Mok CH, Knapp RC, Oike K, Muto MG, Welch WR, Goodman HM, Sheets EE, Berkowitz RS and Lau CC. (1993). *Gynecol. Oncol.*, **48,** 5–10.
Valve E, Martikainen P, Seppanen J, Oksjoki S, Hinkka S, Anttila L, Grenman S, Klemi P and Harkonen P. (2000). *Int. J. Cancer*, **88,** 718–725.
Van Niekerk CC, Ramaekers FCS, Hanselaar AGJM, Aldeweireldt J and Poels LG. (1993). *Am. J. Pathol.*, **142,** 157–177.
von Heydebreck A, Huber W, Poustka A and Vingron M. (2001). *Bioinformatics*, **17,** S107–S114.
Walsh FS and Doherty P. (1997). *Annu. Rev. Cell Dev. Biol.*, **13,** 425–456.
Welsh JB, Zarrinkar PP, Sapinoso LM, Kern SG, Behling CA, Monk BJ, Lockhart DJ, Burger RA and Hampton GM. (2001). *Proc. Natl. Acad. Sci. USA*, **98,** 1176–1181.

Supplementary Information accompanies the paper on Oncogene website (http://www.nature.com/onc).